Decadal variability in North Atlantic phytoplankton blooms

Stephanie A. Henson,[1] John P. Dunne,[2] and Jorge L. Sarmiento[1]

Received 30 September 2008; revised 13 February 2009; accepted 23 February 2009; published 25 April 2009.

[1] The interannual to decadal variability in the timing and magnitude of the North Atlantic phytoplankton bloom is examined using a combination of satellite data and output from an ocean biogeochemistry general circulation model. The timing of the bloom as estimated from satellite chlorophyll data is used as a novel metric for validating the model's skill. Maps of bloom timing reveal that the subtropical bloom begins in winter and progresses northward starting in May in subpolar regions. A transition zone, which experiences substantial interannual variability in bloom timing, separates the two regions. Time series of the modeled decadal (1959–2004) variability in bloom timing show no long-term trend toward earlier or delayed blooms in any of the three regions considered here. However, the timing of the subpolar bloom does show distinct decadal-scale periodicity, which is found to be correlated with the North Atlantic Oscillation (NAO) index. The mechanism underpinning the relationship is identified as anomalous wind-driven mixing conditions associated with the NAO. In positive NAO phases, stronger westerly winds result in deeper mixed layers, delaying the start of the subpolar spring bloom by 2–3 weeks. The subpolar region also expands during positive phases, pushing the transition zone further south in the central North Atlantic. The magnitude of the bloom is found to be only weakly dependent on bloom timing, but is more strongly correlated with mixed layer depth. The extensive interannual variability in the timing of the bloom, particularly in the transition region, is expected to strongly impact the availability of food to higher trophic levels.

Citation: Henson, S. A., J. P. Dunne, and J. L. Sarmiento (2009), Decadal variability in North Atlantic phytoplankton blooms, *J. Geophys. Res.*, *114*, C04013, doi:10.1029/2008JC005139.

1. Introduction

[2] The seasonal cycle of phytoplankton growth is a key driver of the biological carbon pump and the transfer of energy to higher trophic levels. Interannual and decadal variability in the timing and magnitude of phytoplankton blooms is postulated to have significant impacts on, for example, the timing of zooplankton development (e.g., F. Rey et al., Primary production in relation to climate changes in the Barents Sea, paper presented at 3rd Soviet-Norwegian Symposium, Institute of Marine Research, Murmansk, USSR, 1987) and larval fish survival [e.g., *Platt et al.*, 2003]. The classic description of the conditions necessary for phytoplankton bloom initiation was developed by *Sverdrup* [1953] for the subpolar North Atlantic. Deep mixed layers and low sun angle during winter reduce the mean light available to phytoplankton to a level below that required for growth. Winter mixing also determines the nutrient concentration in the euphotic zone that will be available for new production in the following spring [e.g., *Koeve*, 2001]. Increasing incident light and reduced mixing in spring result in the mixed layer shallowing beyond a "critical depth" where the average light intensity is such that phytoplankton growth exceeds losses, and the spring bloom begins. Interannual variability in bloom timing and magnitude will therefore occur through variability in winter and spring mixing conditions. Sverdrup's critical depth model does not, however, apply in subtropical regions, where phytoplankton growth is not seasonally light limited. Instead, relatively shallow mixed layers and high irradiance year-round result in surface nutrient limitation. In these regions, the bloom may actually commence in fall or winter as the mixed layer deepens [e.g., *Dutkiewicz et al.*, 2001; *Siegel et al.*, 2002]. The interplay between light availability and nutrient supply was investigated by *Follows and Dutkiewicz* [2001] who identified two regimes, the subpolar and subtropical, on the basis of the ratio of critical depth to winter mixed layer depth (MLD). Lying between the subpolar and subtropical regimes is a transition zone which may experience either, or both, nutrient and light limitation.

[3] Very few sufficiently long biological time series exist to assess interannual- to decadal-scale variability in the phytoplankton bloom. The exception is the Continuous Plankton Recorder (CPR) program, which consists of a qualitative index of phytoplankton color that indicates relative changes in phytoplankton production [*Reid et al.*, 1998]. Consistent phytoplankton data are available from 1948 onward, and currently the survey consists of monthly

[1] Atmospheric and Oceanic Sciences Program, Princeton University, Princeton, New Jersey, USA.
[2] NOAA Geophysical Fluid Dynamics Laboratory, Princeton, New Jersey, USA.

0148-0227/09/2008JC005139

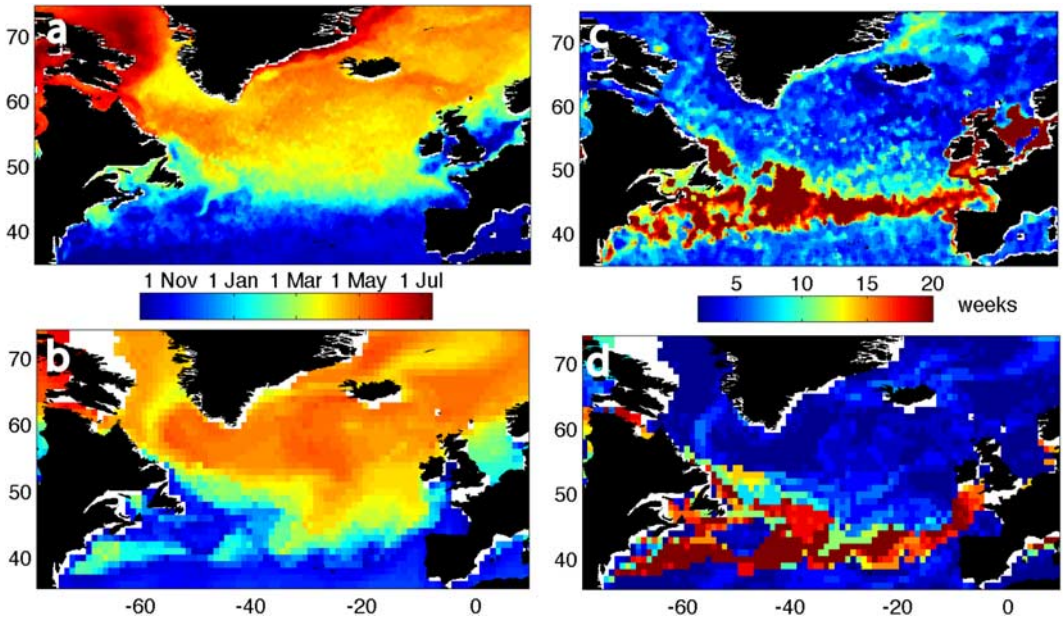

Figure 1. Mean (1998–2004) start date of the phytoplankton bloom estimated from (a) SeaWiFS chlorophyll data and (b) TOPAZ model output. Range in start date (in weeks) from (c) SeaWiFS data and (d) TOPAZ model output.

transects across the major geographical regions of the North Atlantic [*Warner and Hays*, 1994]. The influence of the positive North Atlantic Oscillation (NAO) phase of the late 1980s and early 1990s, and associated strong winds, was found to reduce phytoplankton concentrations on both sides of the North Atlantic. It was also suggested that the onset of the spring bloom would be delayed, however the monthly resolution of the data was insufficient to demonstrate this [*Dickson et al.*, 1988; *Mann and Drinkwater*, 1994; *Edwards et al.*, 2001]. The response was also not spatially consistent across the basin, with the North Sea, Scotian Shelf and Rockall region experiencing increases in CPR color index [*Sameoto*, 2001; *Reid et al.*, 1998; *Edwards et al.*, 2001]. Although correlations between the decadal time series of color index and NAO are barely statistically significant, a clear spatial pattern emerges, with a positive trend occurring in a transition zone in the central North Atlantic [*Barton et al.*, 2003], suggesting that this region is particularly sensitive to changes in basin-scale forcing. Correlations between the NAO and copepod populations or recruitment of larval fish have also been documented [e.g., *Fromentin and Planque*, 1996; *Beaugrand et al.*, 2000; *Ottersen and Stenseth*, 2001; *Brander*, 1994]. The CPR data set is unique in its length, and despite having relatively low-spatial- and temporal-resolution, some analysis of decadal variability in phytoplankton bloom dynamics and the underlying physical forcing has been possible [*Edwards et al.*, 2001; *Beaugrand*, 2004; *McQuatters-Gollop et al.*, 2007].

[4] Interannual and decadal variability in the spatial patterns, timing and magnitude of the annual phytoplankton bloom is partly a response to variability in the underlying physical forcing, and as the global climate continues to change, ocean biology will respond accordingly. Understanding past variability in bloom dynamics and the associated physical mechanisms is key to predicting how ocean biology will respond to climate change. In addition, if we wish to assess to what degree global warming may already be impacting ocean primary production, there is an urgent need to understand the range of "normal" interannual to decadal variability. The 10+ years (September 1997 onward) of consistent Sea-viewing Wide Field-of-view Sensor (SeaWiFS) ocean color data provides an invaluable record of interannual variability, but needs to be placed in a longer-term context to determine whether unprecedented changes to phytoplankton productivity are already occurring. This study uses output from a 3-D physical-biogeochemical model in combination with SeaWiFS data to investigate the decadal (1960–2007) variability in timing and magnitude of North Atlantic phytoplankton blooms and the associated physical mechanisms.

2. Data, Model, and Methods

[5] Level 3 SeaWiFS chlorophyll-a concentration (chl) data (OC4, reprocessing v5.2) for September 1997 to December 2007 were downloaded from http://oceancolor.gsfc.nasa.gov/. All calculations were done with the original 9 km, 8-day-resolution data and were then regridded to 1° resolution to match the model output. (For plotting purposes, SeaWiFS data in Figures 1a, 1c, and S1 are plotted at 1/4° resolution).[1] In the 8-day composites, clouds obscure any particular pixel $\sim$ 20–30% of the time in the high latitudes (in the period March through October), and only about 5–10% of the time in the subtropics. The timing of the annual phytoplankton bloom was estimated the same way for both the SeaWiFS data and model output, using the method of *Siegel et al.* [2002]. The bloom start is defined as the first day of the year on which chl rises 5% above the

[1] Auxiliary materials are available in the HTML. doi:10.1029/2008JC005139.

annual median. For this study, the annual period runs from 1 September to 31 August in order to capture the start of the subtropical bloom, which occurs in autumn. We use the convention that the year which runs from, for example, September 1997 to August 1998 is referred to as 1998.

[6] Optimally interpolated temperature and salinity fields derived from Argo float profiles for the period 2002–2007 were obtained from the Coriolis project (http://www.coriolis.eu.org). Weekly fields at standard depths are produced from all available Argo float profiles using the methodology of *Bretherton et al.* [1976] [*Autret and Gaillard*, 2005]. MLD was estimated as the depth at which the density difference from the surface was >0.125 kg m^{-3}.

[7] We use a biogeochemical and ocean ecosystem model (Tracers for Ocean Phytoplankton with Allometric Zooplankton (TOPAZ)), developed at the National Oceanic and Atmospheric Administration's Geophysical Fluid Dynamics Laboratory (GFDL), which is integrated with the MOM-4 ocean model [*Griffies et al.*, 2004; *Gnanadesikan et al.*, 2006]. MOM-4 is forced with the Common Ocean-Ice Reference Experiment (CORE) forcing data set that covers the period 1959–2004 [*Large and Yeager*, 2004]. MOM-4 has 50 vertical z-coordinates and spatial resolution is nominally 1° globally, with higher 1/3° resolution near the equator. The model is forced with a mixed boundary coupler through a dynamic sea ice model with active estimation of outgoing fluxes of freshwater and longwave radiation. Incoming fluxes of wind stress, freshwater flux, shortwave and longwave radiation are prescribed as boundary conditions from the CORE version 1 reanalysis effort [*Large and Yeager*, 2004]. The representation of interannual variability in the model includes near-surface wind speed, air temperature and relative humidity, all of which are available from 1959 onward, allowing interannually varying calculations of the air-sea turbulent fluxes. For the other input parameters, interannual data is available only for a portion of the full period and data gaps are filled with the climatological annual cycle. Radiative components of the air-sea flux are available from 1983, and precipitation since 1979. Runoff is only available as a climatological annual value, and so contains no information on seasonal or interannual variability. There is ongoing salinity restoring at each time step in the model, which dampens the interannual variability in MLD somewhat. Despite this, the physical model displays distinct interannual signals, which propagate through to the biogeochemical component of the model. The model was run 7 times on a 46-year loop and output was saved as 8-day means from the final loop.

[8] The TOPAZ biogeochemical model is designed to reproduce diverse interactions between the marine ecosystem and the physical environment as accurately as possible, while incorporating as little complexity as possible. The model has been tested and calibrated against global nutrient and satellite observations in the GFDL global, 1°-resolution ocean model. All major nutrient elements are considered (N, P, Si and Fe), and the model includes both labile and semilabile dissolved organic pools, along with parameterizations to represent the microbial loop. Growth rates are modeled as a function of variable chlorophyll to carbon ratios and are colimited by nutrients and light. Photoacclimation is based on the *Geider et al.* [1997] algorithm, extended to account for colimitation by multiple nutrients and including a parameterization for the role of iron in phytoplankton physiology (following *Sunda and Huntsman* [1997]). Loss terms include zooplankton grazing and ballast-driven particle export. Remineralization of detritus and cycling of dissolved organic matter are also explicitly included [*Dunne et al.*, 2005]. The model also traces dissolved oxygen, DIC and alkalinity, and includes highly flexible phytoplankton stoichiometry and variable chl:C ratios. Three classes of phytoplankton form the base of the global ecosystem. "Small" phytoplankton represent cyanobacteria and picoeukaryotes, resisting sinking and tightly bound to the microbial loop. "Large" phytoplankton represent diatoms and other eukaryotic phytoplankton, which sink more rapidly. "Diazotrophs" fix nitrogen directly rather than requiring dissolved forms of nitrogen. All phytoplankton are simultaneously limited by the availability of light and multiple nutrients, but each class has its own set of tunable parameters for determining growth rates and its own nutrient stoichiometry. Wet and dry dust deposition fluxes are prescribed from the monthly climatology of *Ginoux et al.* [2001] and converted to soluble iron using a variable solubility parameterization [*Fan et al.*, 2006]. TOPAZ includes a simplified version of the oceanic iron cycle including biological uptake and remineralization, particle sinking and scavenging and adsorption/desorption.

3. Results

3.1. Data-Model Comparison of Bloom Timing

[9] The mean (1998–2004) phytoplankton bloom start date as estimated from SeaWiFS chl data is plotted in Figure 1a. (Plots of the start date in each individual year 1998–2007 can be found in Figure S1). The model estimated mean (1998–2004) bloom start date is plotted in Figure 1b. The key features observed in the satellite data are reproduced by the model. In the subtropical region, south of $\sim$ 45 °N, the bloom begins between October and December in both the model and data. The start of the bloom progresses northward approximately zonally between $\sim$ 45 and 55 °N, beginning between March and April. The principal difference between data and model occurs east of the Gulf of St. Lawrence, where the modeled bloom occurs in November, compared to February–March in the data. This reflects a Gulf Stream which separates too far south in the physical model [*Gnanadesikan et al.*, 2006]. Over shallow shelf regions, such as the North and Celtic Seas, the bloom starts earlier than in the open ocean at an equivalent latitude, in $\sim$ December–January. North of 55 °N the latitudinal gradient in timing disappears and the spring bloom starts patchily across the entire region between $\sim$ mid-April and mid-May (the same phenomenon is also observed in CPR data [e.g., *Reid*, 2005]). In the seasonally ice-covered regions of Baffin Bay and the eastern Greenland coast, the bloom starts in July in the SeaWiFS data. This arises either because SeaWiFS cannot observe the ocean surface until the ice melts, or because the phytoplankton bloom is genuinely associated with the retreating edge of seasonal sea ice [*Mei et al.*, 2002; *Waniek et al.*, 2005]. Off the west coast of Greenland, there is a triangle-shaped area of relatively early bloom timing in the SeaWiFS data, and to a lesser extent in the model output. Freshwater melt from Greenland, advected offshore by the West Greenland Current, prompts

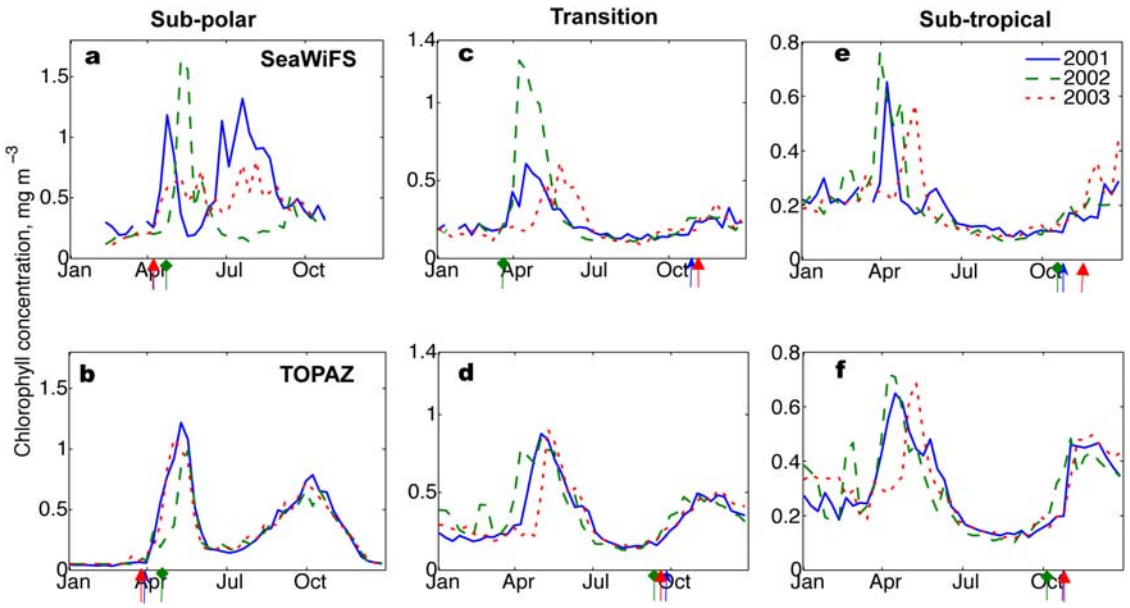

Figure 2. Example time series of chlorophyll concentration (mg m^{-3}) in 2001 (solid line), 2002 (dashed line), and 2003 (dotted line) in the (a, b) subpolar, (c, d) transition, and (e, f) subtropical regions from SeaWiFS data (Figures 2a, 2c, and 2e) and TOPAZ model output (Figures 2b, 2d, and 2f). Time series are means of 1° boxes, centered at 56.5 °N, −20.5 °W (subpolar); 40.5 °N, −40.5 °W (transition); and 37.5 °N, −39.5 °W (subtropical). Arrows mark estimated start of the bloom, where v-shaped arrows indicate 2001, flat arrowheads indicate 2002, and diamond arrowheads indicate 2003.

an early bloom in ∼ April (E. Frajka-Williams and P. B. Rhines, Physical controls on the interannual variability of the Labrador Sea phytoplankton bloom using Sea-viewing Wide Field-of-View Sensor (SeaWiFS), submitted to *Deep Sea Research, Part II*, 2009). Another area of relatively early bloom timing extends northeast of Iceland. The East Iceland Current, which is colder and fresher than surrounding waters, stratifies earlier in spring [*Gaard and Nattestad*, 2002], apparently prompting an early phytoplankton bloom.

[10] The contrasting seasonality in chl in the subpolar, transition and subtropical regimes is demonstrated in Figure 2 (definition of the regimes will be formally introduced in the following section). Typical subpolar, transition and subtropical chl time series for the example years 2001, 2002 and 2003 are plotted. In the subpolar example from SeaWiFS data (Figure 2a), chl rises rapidly in mid-April to ∼ 1–1.5 mg m^{-3} from a winter value of ∼ 0.2 mg m^{-3}. The bloom starts each year on ∼ 20 April ± 10 days, but the subsequent development of the bloom varies greatly interannually. In this example, the summer minimum following the peak of the bloom occurs ∼ 80 days later in 2002 than in 2001, whereas in 2003, spring and fall bloom peaks are indistinct. In the subpolar region, the model reproduces the timing of the spring bloom, and the interannual variability in timing, however the fall peak is much later (by ∼ 80 days) than in the SeaWiFS data (Figure 2b). The interannual variability in bloom development is not well reproduced. The modeled seasonal cycle follows a similar cycle each year, whereas in the satellite data bloom development is highly variable. The model does not resolve mesoscale processes and has a relatively simple zooplankton grazing scheme, both of which may contribute to the lack of variability in modeled chl seasonality.

[11] The example time series for the transition region (Figures 2c and 2d) show that the mean magnitude of chl is similar in the SeaWiFS data and TOPAZ output, although the interannual variability is more pronounced in the data than in the model. In the SeaWiFS data (Figure 2c) the bloom start was estimated to occur in autumn in 2001 and 2003 and the bloom magnitude is similar to subtropical concentrations. In 2002, however, the bloom start was estimated to be ∼ mid-March and the peak chl concentrations are representative of the subpolar region.

[12] In the subtropical example from SeaWiFS (Figure 2e), the bloom starts in autumn/winter ∼ 1 November ± 10 days. Chl slowly rises from summer concentrations of ∼ 0.1 mg m^{-3}, with a sharp increase to peak values of ∼ 0.5 mg m^{-3} in early April. The model successfully reproduces the seasonal variability of the subtropical chl (Figure 2f). The timing of the bloom start in autumn and the peak values in ∼ April match the SeaWiFS data well. The interannual variability in the seasonal cycle and magnitude of chl is also well captured in the model.

[13] Regional differences in the interannnual variability of bloom timing are illustrated by the range in start dates (latest minus earliest) plotted in Figure 1c. In the subpolar and subtropical regions interannual variability is relatively low (range of ∼ 2–3 weeks), although still large enough to potentially impact the development of zooplankton and fish larvae [*Cushing*, 1990]. The greatest interannual variability occurs in the transition zone (∼ 20 weeks), which is widest in the western basin (∼ 10° of latitude) and narrows to a thin band to the east (∼ 2° of latitude). The range in bloom timing in the model output is similar to that of the SeaWiFS data, with the transition zone lying at the correct latitude and narrowing across the basin from west to east (Figure 1d).

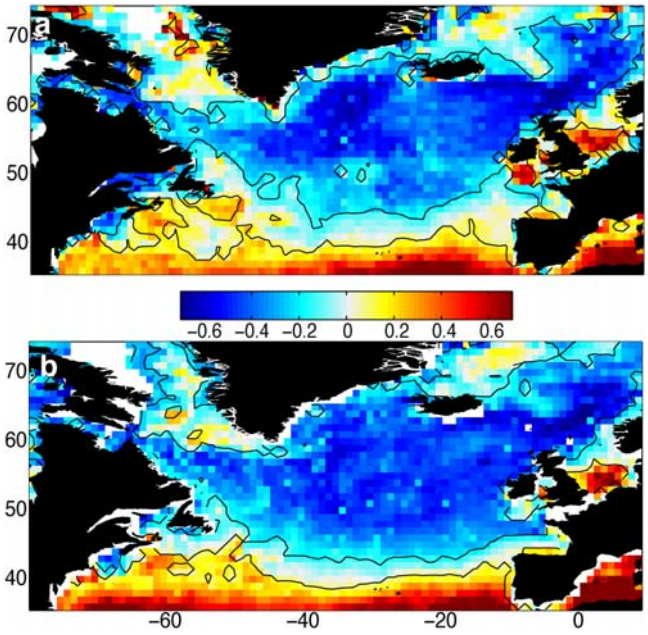

Figure 3. Temporal correlation coefficient between weekly SeaWiFS chlorophyll concentration and (a) MLD estimated from optimally interpolated Argo float data and (b) modeled MLD. Black contour marks regions where correlation is significant at the 95% level.

Here, the bloom may either start in spring and have peak values representative of the subpolar bloom or start in autumn and have characteristics similar to the subtropical bloom (Figures 2c and 2d).

3.2. Response to Mixed Layer Depth Seasonality

[14] Phytoplankton growth in the subpolar region is seasonally light-limited (during winter, modeled mean depth-averaged irradiance is <21 W m^{-2}, the theoretical lower limit for phytoplankton growth [*Riley*, 1957]). However, phytoplankton growth in the subtropical region is nutrient limited (climatological annual nitrate concentrations are <1 μmol l^{-1} [*Garcia et al.*, 2006]). This dichotomy is encapsulated in the relationship between chl and MLD. The correlation coefficient between weekly SeaWiFS chl and mapped MLD estimated from Argo float data (for the period 2002–2007) is plotted in Figure 3a. The correlation between modeled MLD and SeaWiFS chl for the period 1998–2004 is plotted in Figure 3b. Because of the strong seasonality in both chl and MLD, and autocorrelation within both time series, the correlation coefficients are artificially high. The results are therefore used only to define the geographic location of the transition from positive to negative correlation. The spatial pattern of positive and negative correlation, as well as the regions of nonsignificant correlation, are similar in both the model- and data-based analyses. In the subpolar region, the negative correlation is consistent with light limitation of phytoplankton growth, so that chl increases rapidly in spring as the mixed layer shallows and returns to winter concentrations as the mixed layer deepens in autumn. The positive correlation in the subtropics reflects the nutrient limitation of this region which is alleviated as the mixed layer deepens in autumn, prompting an increase in chl. Small correlation coefficient values in the transition zone indicate that there is no interannually consistent chl response to seasonally changing MLD, i.e., the bloom may have either subpolar or subtropical characteristics. This transition region overlies the area of high interannual variability in bloom timing identified in Figures 1c and 1d. Low correlation coefficients are also found to the west of Greenland and northeast of Iceland, the areas identified as experiencing relatively early blooms (Figure 1a). As a result of freshwater input, thin surface layers of increased stability can form prior to the establishment of the seasonal thermocline [e.g., *Waniek et al.*, 2005], leading to the observed lack of correlation between chl and MLD.

[15] A transition zone between subpolar and subtropical regimes was noted by *Follows and Dutkiewicz* [2001] who used an argument based on seasonal light availability. The ratio of the climatological Sverdrup critical depth to winter MLD separated the basin into two provinces with a transition region between them at $\sim$ 30–35 °N. In the eastern North Atlantic, *Levy et al.* [2005] used the seasonal characteristics of SeaWiFS chl to define a "midlatitude" region at $\sim$ 35–40 °N. The transition region defined here on the basis of chl response to seasonal MLD and bloom timing lies somewhat further north than either of these two definitions, at $\sim$ 40–45 °N.

[16] For the following analyses the subpolar, transition and subtropical zones are defined on the basis of the sign of the chl-MLD correlation (as per Figure 3). Coastal areas, shelf seas, the Mediterranean Sea and seasonally ice-covered regions are excluded from the analysis. The subpolar region is defined as the area where the correlation between MLD and chl is negative and $p < 0.05$; the subtropical region is where the correlation is positive and $p < 0.05$; and the transition zone is the area where MLD and chl are seasonally uncorrelated.

3.3. Decadal Variability in Bloom Timing

[17] The decadal time series (1960–2007) of bloom timing, presented as anomalies from the mean, are plotted in Figure 4 for each of the three regions. The mean start dates for the subpolar, transition and subtropical zones are 11 April, 29 December, and 23 November, respectively. The range in bloom timing is greatest in the transition zone ($\pm\sim$ 50 days), and relatively small in the subpolar region ($\pm\sim$ 15 days). None of the regions displays any long-term trend in bloom timing. In the subpolar region however, there are consistent decadal-scale fluctuations in bloom timing, so that from $\sim$ 1969–1990 there is a gradual change from the bloom starting $\sim$ 10 days earlier than the mean ($\sim$ early April) to starting $\sim$ 10 days later than the mean ($\sim$ late April). After being consistently $\sim$ 10 days later than the mean during the period 1985–1995, bloom timing returns to approximately its mean value through the end of the time series. Neither the transition or subtropical regions exhibit similar decadal-scale fluctuations in bloom timing.

[18] As the start of the subpolar bloom relies on the spring shallowing of the MLD (Figure 3), the decadal-scale variability likely reflects changes in the physical environment. The dominant mode of atmospheric and oceanic variability in this region is the North Atlantic Oscillation (NAO) [*Hurrell*, 1995]. The NAO has well-known effects

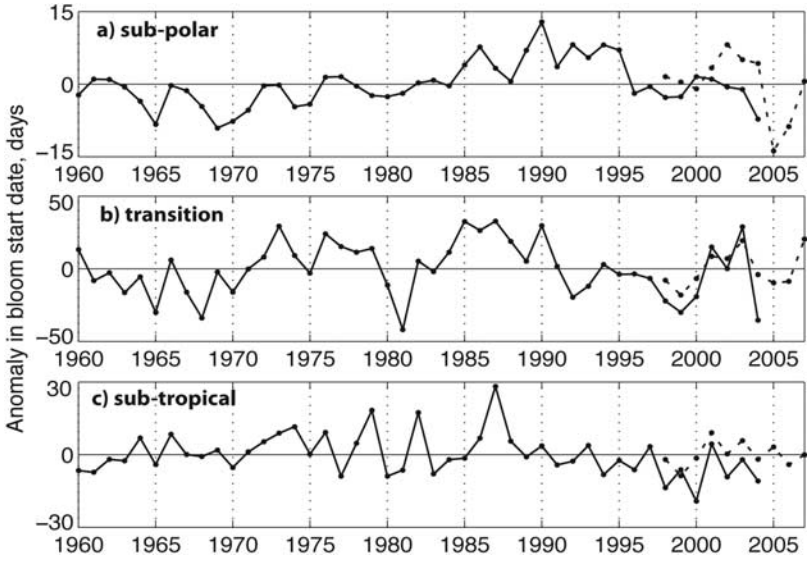

Figure 4. Time series from 1960 to 2007 of the bloom start date presented as anomalies from the mean in the (a) subpolar, (b) transition, and (c) subtropical regions calculated from TOPAZ model output (solid line) and SeaWiFS data (dashed line). The mean start dates for the subpolar, transition, and subtropical zones are 11 April, 29 December, and 23 November, respectively.

on the strength of westerly winds, storm tracks, and hence upper ocean heat exchange and rainfall patterns [e.g., *Visbeck et al.*, 2003]. The differences in mean modeled zonal wind stress and MLD between a period of consistently positive NAO (1988–1995) and negative NAO (1962–1966) are plotted in Figures 5a and 5b, respectively. The westerly wind stress is strongly intensified over the subpolar region, particularly south of Greenland and Iceland. As a result, MLD in the subpolar region is 100–300 m deeper in positive NAO periods than in negative ones. In the Labrador Sea, modeled MLD deepens by several hundred meters south of Greenland, and shallows to a similar degree to the northwest. This reflects an expansion of the region of deep convective mixing (cf. for example, *Mignot and Frankignoul* [2005]) and a shift in the center of action to the southeast during positive NAO years.

[19] The consequences for subpolar bloom timing are shown in Figure 6, where the time series of subpolar bloom start dates is plotted against the mean annual MLD and NAO index for 1960–2004. Periods of deeper MLD coincide with positive NAO index and later bloom timing, and vice versa. Linear correlation coefficients are $r = -0.76$ ($p < 0.05$) for bloom timing against MLD and $r = 0.61$ ($p < 0.05$) for the NAO index. In positive NAO periods, the annual mean MLD in the subpolar region is up to 65 m deeper than the long-term average and the bloom is delayed by up to 2 weeks. Timing of the transition and subtropical region blooms is not significantly correlated with the NAO.

[20] The basin-wide difference in bloom timing between a period of persistent positive NAO (1988–1995) and the mean is shown in Figure 7a. In positive NAO years, the subpolar bloom is $\sim$ 10–20 days later than the mean in the area south of Greenland. Maximum positive anomalies of $\sim$ 50 days are found in the eastern central basin in a band stretching southeastward from $\sim$ 50 °N, 55 °W to 40 °N, 35 °W. The bloom starts $\sim$ 30–40 days earlier in positive NAO years in a band centered $\sim$ 40 °N. The spatial variability in bloom timing anomalies in the subpolar region is similar to the MLD anomalies shown in Figure 5b. In particular, the deeper mixed layers of the western basin are reflected in later bloom timing, and vice versa in the eastern portion of the subpolar region. A similar spatial pattern, but with opposite sign anomalies, occurs in negative NAO years (Figure 7b).

[21] A schematic of the changes in spatial extent of the bloom regions during a positive and negative NAO phase is presented in Figure 8. Under mean conditions (Figure 8a), a

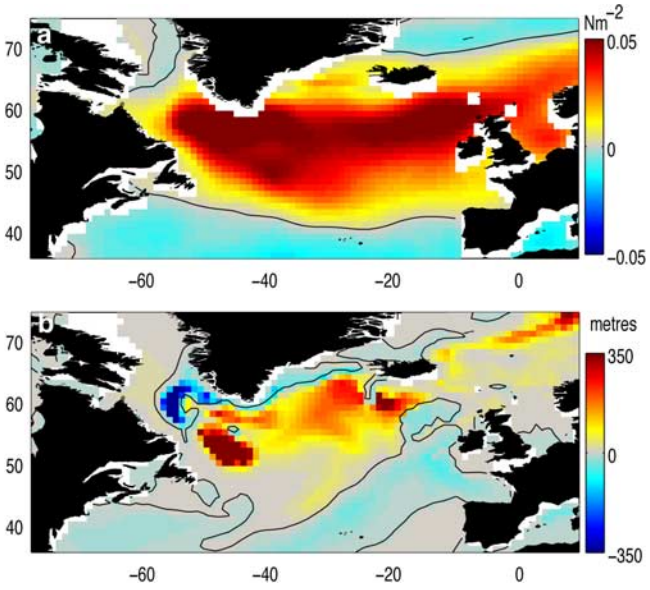

Figure 5. Difference in (a) annual mean Common Ocean-Ice Reference Experiment forcing zonal wind stress and (b) annual mean modeled mixed layer depth between a positive NAO phase (1988–1995) and a negative phase (1962–1966). The zero line is marked by the black contour.

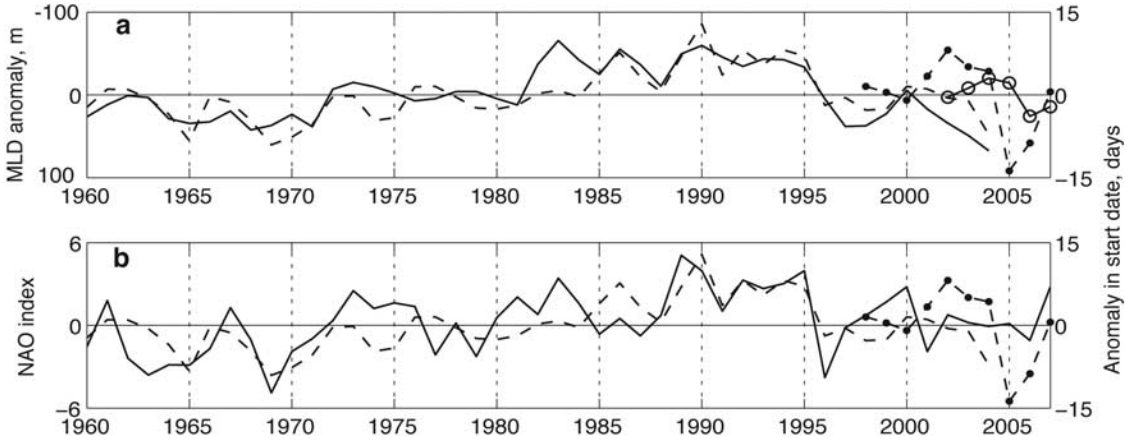

Figure 6. Time series of modeled subpolar bloom start date (dashed line) and SeaWiFS-derived start date (dashed line with dot markers) and (a) annual mean modeled MLD (solid line) and Argo float-derived MLD (solid line with circle markers), plotted as anomalies from the mean (note reversed axis), and (b) NAO index (solid line). Linear correlation coefficients are −0.76 and 0.61, respectively ($p < 0.05$ in both cases).

latitudinal gradient in bloom timing exists, with the transition region oriented zonally at ∼ 45 °N. In positive NAO years (Figure 8b), increased westerly wind stress results in deeper MLD and extends the boundary of the subpolar zone further south between ∼ 25 and 50 °W. The bloom in this area, which under normal conditions lies in the transition zone, behaves instead like the subpolar bloom, resulting in the bloom timing shifting from ∼ January to March. The northern boundary of the subtropical region shifts northward on both sides of the basin. The bloom, which under normal conditions is representative of the transition zone, switches to the subtropical region and an earlier bloom start (from ∼ January to November). Under positive NAO conditions, the transition zone becomes narrower and bows southward in the western central basin and northward at the edges, particularly in the eastern Atlantic, where subtropical conditions extend northeastward toward the British Isles. In negative NAO years, the opposite spatial pattern is observed with a bowing northward of the transition zone in the central basin (Figure 8c). A portion of the region which normally has bloom timing typical of the subpolar zone becomes encompassed by the transition region.

3.4. Impact of Timing on Bloom Magnitude

[22] Substantial interannual and decadal variability in bloom timing occurs, but does this have any impact on the magnitude of the subsequent bloom? Plots of the mean start date in each year against the modeled mean annual chlorophyll for each of the three regions show weak correlations (data not shown). In the subpolar region, $r = -0.26$ ($p < 0.1$), in the subtropics, $r = 0.29$ ($p < 0.1$) and in the transition region there is no significant correlation. The negative (positive) correlation in the subpolar (subtropical) region is consistent with light (nutrient) limitation of the phytoplankton bloom. In the subtropical region, the trend is for a late start to result in increased bloom magnitude. A delayed bloom is indicative of deeper mixed layers, and therefore increased surface nutrient concentrations. At high latitudes, seasonally light limiting conditions may result in a late starting bloom being curtailed by a short growing season. Alternatively, a late starting bloom may result in increased grazing pressure, as zooplankton have had longer to reproduce, thus limiting the magnitude of the spring phytoplankton bloom [*Colebrook*, 1979; *Gifford et al.*, 1995]. Unfortunately, this hypothesis cannot be tested with

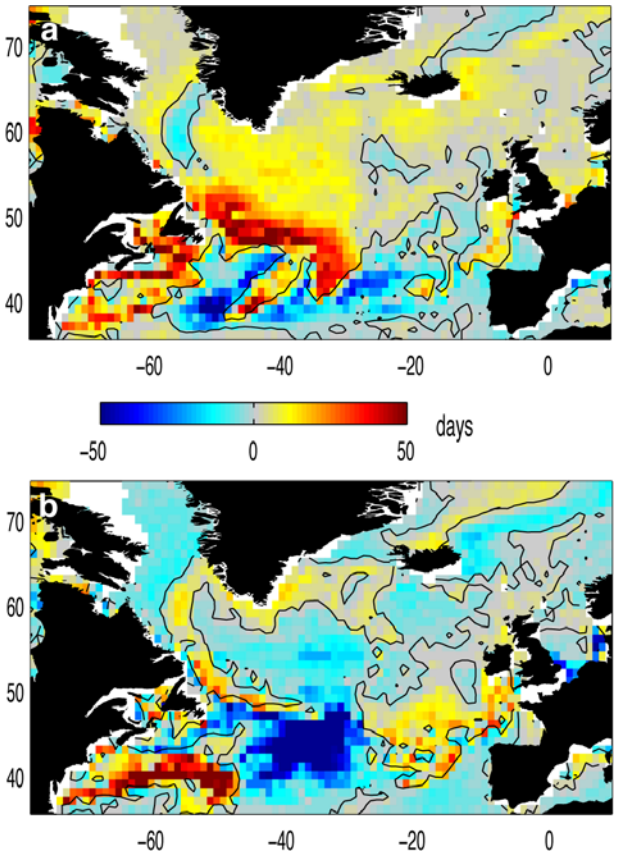

Figure 7. Difference in bloom start date (days) between the long-term mean (1960–2004) and (a) a positive NAO phase (1988–1995) and (b) a negative NAO phase (1962–1966). The zero line is marked by the black contour.

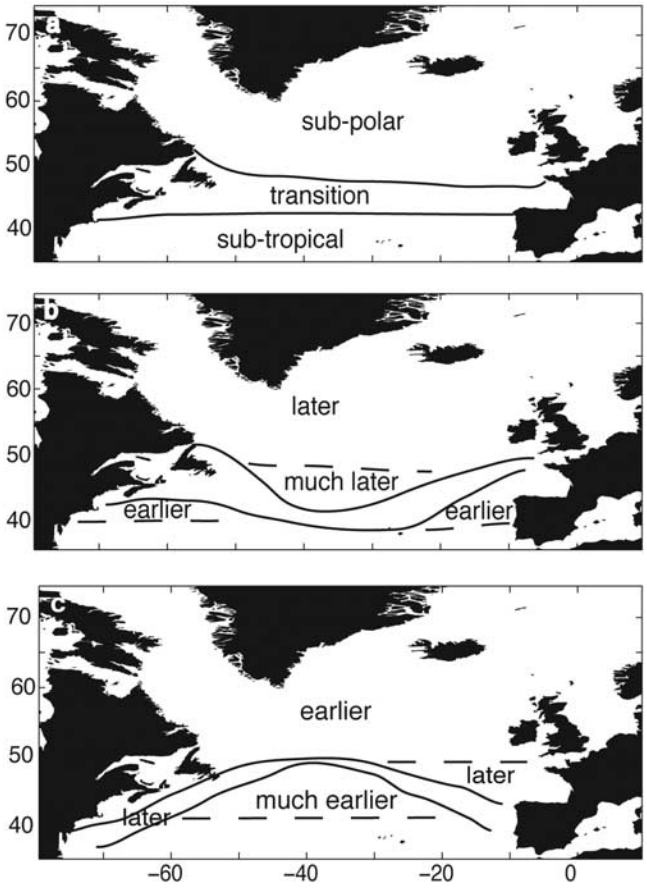

Figure 8. Sketch of the locations of the three bloom regions under (a) mean conditions, (b) in a positive NAO phase, and (c) in a negative NAO phase (dashed line marks position of transition region under mean conditions). The nature of the response in bloom timing is marked.

the TOPAZ model, which currently parameterizes zooplankton grazing as a simple loss term, i.e., the zooplankton biomass and seasonal cycle is determined by the phytoplankton biomass and seasonal cycle. Thus, examining the biomass of the two groups provides no additional insight into ecosystem interactions.

[23] Although bloom magnitude is not well correlated with bloom timing, there is a moderately strong relationship with modeled MLD (Figure 9). In the subpolar region deeper mixed layers are associated with weaker blooms ($r = -0.48$, $p < 0.05$). Deep mixing will entrain more nutrients into the euphotic zone; however, the controlling factor on subpolar blooms is likely to be light availability, so that increased mixing results in a delayed, low-magnitude bloom. In the subtropical region, where nutrient limitation of the phytoplankton bloom prevails, increased mixing results in increased bloom magnitude ($r = 0.49$, $p < 0.05$). The lack of a relationship in the transition region confirms that there are no interannually consistent bloom dynamics: the bloom may have either subpolar or subtropical characteristics, as the subtropical gyre edge migrates latitudinally.

[24] The timing of the bloom is tightly coupled to MLD. The magnitude of the bloom is moderately correlated with the MLD, but only weakly correlated to bloom timing. The lack of a clear relationship between bloom timing and magnitude in the North Atlantic was also noted by *Levy et al.* [2005], *Henson et al.* [2006], and *Bennington et al.* [2009]. This suggests that while bloom timing is strongly driven by physical forcing processes, the magnitude of the bloom is determined by a combination of physical forcing and other factors, such as zooplankton grazing, phytoplankton species succession, self-shading etc.

4. Discussion

[25] Our results demonstrate that substantial interannual and decadal variability in the timing of phytoplankton blooms occurs in the North Atlantic in response to variability in basin-scale forcing. The TOPAZ model is able to accurately reproduce the timing of the annual phytoplankton bloom, as observed in SeaWiFS data. Bloom timing has proven to be a very useful metric of model skill, as it reflects hydrography and circulation features, in addition to bloom dynamics. Although the well-known correlations between the phase of the NAO and atmospheric conditions have long been hypothesized to affect phytoplankton blooms [e.g., *Mann and Drinkwater*, 1994], the lack of high-resolution, consistent, long-term biological records has presented difficulties in investigating the relationships. This study, by using a combination of model output and satellite data, quantifies the decadal variability in bloom timing and magnitude, its spatial variability, the underlying physical mechanisms and the impact of the NAO on biological productivity in the North Atlantic.

[26] Positive NAO conditions, associated with intensified westerly winds and deeper mixed layers, result in later blooms in the central subpolar region, and also cause the transition zone to shift latitudinally. It is not, however, a simple north-south movement. Instead, the subpolar region is bowed southward and the subtropical gyre extends northward on either side of the Atlantic. The northeast extension of the subtropical gyre (as defined by transport

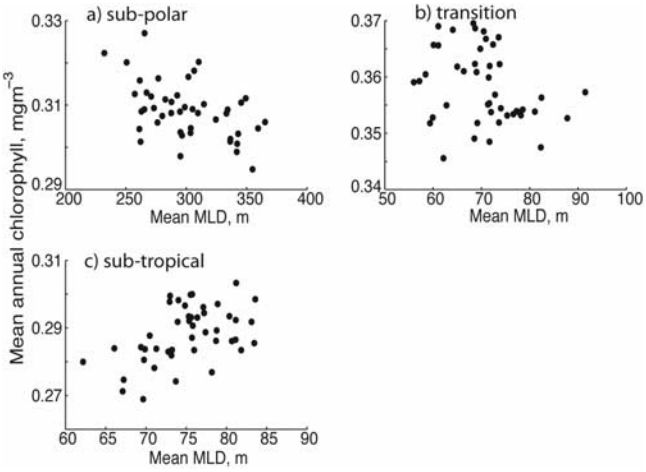

Figure 9. Mean annual modeled chlorophyll plotted as a function of mean annual MLD for the (a) subpolar, (b) transition, and (c) subtropical regions. Linear correlation coefficients are -0.48 ($p < 0.05$) and 0.49 ($p < 0.05$) for the subpolar and subtropical regions, respectively. Correlation coefficient for the transition region is not statistically significant.

anomalies, rather than bloom timing) in positive NAO years has been noted by, e.g., *Marshall et al.* [2001]. It appears that this change in the circulation is also reflected in the phytoplankton bloom dynamics (this study) and a northerly movement of zooplankton species [*Beaugrand et al.*, 2008]. The substantial interannual variability in the latitude and spatial extent of the transition zone may have implications for the efficiency of the biological carbon pump [*Levy et al.*, 2005]. The transition zone overlies the region of winter time mode-water subduction in the Northeast Atlantic. *Levy et al.* [2005] suggest that any primary production which occurs in these waters during autumn/winter will be exported very efficiently. Thus if the bloom starts in spring, and the majority of the annual primary production occurs then, rather than in winter during mode-water subduction, export efficiency may be reduced.

[27] Interannual variability in the position of the transition zone will also have significant impacts on higher trophic levels, as the phytoplankton bloom may start there either in winter or in spring. Even the 2–3 week variability in bloom timing in the subpolar and subtropical regions is likely to impact the survival rates of herbivorous zooplankton and fish. Cushing's match-mismatch hypothesis [*Hjort*, 1914; *Cushing*, 1975] states that the timing of food availability may be as important, or even more so, than the abundance of food. If a mismatch in timing between food availability and critical life stages of higher trophic levels occurs, their survival rate is likely to be reduced. A change in the dominant plankton species in a region could also affect higher trophic level populations [e.g., *Edwards and Richardson*, 2004]. In the North Atlantic, variability in the timing of the phytoplankton spring bloom could be critical to the population of *Calanus finmarchicus*, the most abundant zooplankton species in the region. *C. finmarchicus* diapauses at depths of 400–2000 m in winter [e.g., *Heath et al.*, 2008], ascending to the surface in spring. Food availability is critical to survival during naupliar development, and the subsequent transition to late stage copepodites [*Hirche et al.*, 2001; *Ohman and Hirche*, 2001]. Investigating relationships between interannual to decadal variability in North Atlantic zooplankton populations and the NAO has been possible with the CPR survey data. The long-term, large-scale patterns of variability suggest that climatic factors most likely drive interannual variability in abundance [*Aebischer et al.*, 1990; *Cushing*, 1990; *Beaugrand et al.*, 2008]. Significant correlation between the NAO index and *C. finmarchicus* abundance was suggested by *Fromentin and Planque* [1996] for the North Sea and northeastern Atlantic, although the relationship subsequently broke down [*Planque and Reid*, 1998]. The negative relationship was associated with higher wind stress in positive NAO conditions, resulting in reduced stratification and lower phytoplankton concentrations. Changes in circulation and water temperature associated with the NAO have also been implicated in the interannual and decadal variability in zooplankton populations [*Planque and Taylor*, 1998; *Heath et al.*, 1999; *Beaugrand et al.*, 2000; *Greene and Pershing*, 2000]. Recruitment of larval fish may also be determined by food availability during the critical period of larval development. For example, a bloom starting 3 weeks earlier than usual was associated with a fivefold increase in the survival rate of larval haddock on the Scotian Shelf [*Platt et al.*, 2003]. As the timing of food availability appears to exert significant control on the success of zooplankton and larval fish populations, the substantial interannual variability in phytoplankton bloom timing observed in our results implies that part of the mechanism linking the NAO index and zooplankton abundance may be related to the timing of food availability during critical developmental stages.

[28] With continued global warming, sea surface temperatures are expected to increase, and mixed layers to shoal. Using interannual variability as an analog for climate change, the consequences for primary production of variability in stratification were explored in the 10-year SeaWiFS record by *Behrenfeld et al.* [2006]. In the subtropics, global primary production was shown to decrease because of enhanced stratification and thus nutrient limitation. Consistent with this, our study suggests that shallower mixed layers will result in reduced magnitude blooms in the subtropical region. In the subpolar region, however, production is expected to increase because of alleviation of light limitation and a longer growing season [*Doney*, 2006]. Again consistent with this hypothesis, our study suggests that in the North Atlantic shallower mixed layers will result in earlier bloom timing and enhanced magnitude blooms in the subpolar region. However, decreased mixing in the subpolar region will only result in enhanced bloom magnitude provided winter mixing is deeper than the nutricline (currently $\sim$ 100 m depth). If the result of global warming is that in each successive winter the maximum MLD is shallower, there could come a point when euphotic zone nutrients were not being sufficiently replenished and the subpolar region would become increasingly subtropical in nature. This scenario however assumes that winter storm patterns will also change so that deep mixing events due to storms are not able to entrain sufficient nutrients to fuel the spring bloom.

[29] In the subpolar North Atlantic, warming temperatures will act in opposition to another predicted consequence of increased greenhouse gases: that the NAO index will strengthen under global warming conditions [*Gillett et al.*, 2003]. Most coupled climate models forecast increasingly positive NAO conditions [e.g., *Osborn*, 2002; *Gillett et al.*, 2002], possibly combined with a shift of the center of action northeastward [*Ulbrich and Christoph*, 1999]. Our results suggest that a positive trend in the NAO index will result in increased mixing, and hence a later, weaker bloom in the subpolar North Atlantic. In addition, a shift in the latitudinal position of the transition zone may occur, with blooms in regions either side of the basin at $\sim$ 40 °N becoming more subtropical in nature, i.e., the subtropical gyre would expand. This effect is postulated to be already observable in satellite data [*McClain et al.*, 2004; *Polovina et al.*, 2008], but note that these time series are just 6 and 9 years long, respectively, i.e., not long enough to distinguish a global warming-driven trend from decadal variability.

[30] Only a part of the variability in bloom magnitude is explained by variability in MLD, suggesting that changes in biological factors such as grazing or phytoplankton community composition will also be important in setting the biological response to global warming. The potential response also depends on how quickly environmental conditions change and whether phytoplankton and their predators can adapt sufficiently rapidly. As emphasized by

Boyd et al. [2008], changing conditions with no prevailing trend, such as natural interannual variability, are unlikely to result in wholesale alteration of oceanic ecosystems. However, detecting future changes to ocean biology requires knowledge of the range of current conditions, and analysis of past interannual to decadal variability in phytoplankton populations provides that baseline. It also provides insight into the physical mechanisms behind the variability, understanding of which is essential to predicting how future climate change may impact oceanic primary production. Although biogeochemical models are an invaluable tool for this task, the continuing availability of consistent satellite ocean color data is absolutely central to detecting and monitoring the effects of climate change on ocean biology.

[31] **Acknowledgments.** SeaWiFS data were provided by GSFC/NASA in accordance with the SeaWiFS Research Data Use Terms and Conditions Agreement. Argo float data were collected and made freely available by the International Argo Project and supplied by the Coriolis project. NAO index data were provided by the Climate Analysis Section, NCAR, Boulder. This work was funded by NASA grant NNG06GE77G to J.L.S.

References

Aebischer, N. J., J. C. Coulson, and J. M. Colebrook (1990), Parallel long-term trends across 4 marine trophic levels and weather, *Nature*, *347*, 753–755, doi:10.1038/347753a0.

Autret, E., and F. Gaillard (2005), Système opérationnel d'analyse des champs de température et de salinité mis en œuvre au centre de données CORIOLIS Version 3.03, configuration GLOBAL05 V1.0, report, 63 pp., Inst. Fr. de Rech. pour l'Exploit. de la Mer, Brest, France.

Barton, A. D., C. H. Greene, B. C. Monger, and A. J. Pershing (2003), The Continuous Plankton Recorder survey and the North Atlantic Oscillation: Interannual- to multidecadal-scale patterns of phytoplankton variability in the North Atlantic Ocean, *Prog. Oceanogr.*, *58*, 337–358, doi:10.1016/j.pocean.2003.08.012.

Beaugrand, G. (2004), The North Sea regime shift: Evidences, causes, mechanisms and consequences, *Prog. Oceanogr.*, *60*, 245–262, doi:10.1016/j.pocean.2004.02.018.

Beaugrand, G., F. Ibanez, and P. Reid (2000), Spatial, seasonal and long-term fluctuations of plankton in relation to hydroclimatic features in the English Channel, Celtic Sea and Bay of Biscay, *Mar. Ecol. Prog. Ser.*, *200*, 93–102, doi:10.3354/meps200093.

Beaugrand, G., M. Edwards, K. Brander, C. Luczak, and F. Ibanez (2008), Causes and projections of abrupt climate-drive ecosystem shifts in the North Atlantic, *Ecol. Lett.*, *11*, 1157–1168.

Behrenfeld, M. J., R. T. O'Malley, D. A. Siegel, C. R. McClain, J. L. Sarmiento, G. C. Feldman, A. J. Milligan, P. G. Falkowski, R. M. Letelier, and E. S. Boss (2006), Climate-driven trends in contemporary ocean productivity, *Nature*, *444*, 752–755, doi:10.1038/nature05317.

Bennington, V., G. A. McKinley, S. Dutkiewicz, and D. Ullman (2009), What does chlorophyll variability tell us about export and air-sea CO_2 flux variability in the North Atlantic?, *Global Biogeochem. Cycles*, doi:10.1029/2008GB003241, in press.

Boyd, P. W., S. C. Doney, R. Strzepaek, J. Dusenberry, K. Lindsay, and I. Fung (2008), Climate-mediated changes to mixed layer properties in the Southern Ocean: Assessing the phytoplankton response, *Biogeosciences*, *5*, 847–864.

Brander, K. M. (1994), The location and timing of cod spawning around the British Isles, *ICES J. Mar. Sci.*, *51*, 71–89, doi:10.1006/jmsc.1994.1007.

Bretherton, F. P., R. E. Davis, and C. B. Fandry (1976), Technique for objective analysis and design of oceanographic experiments applied to MODE-73, *Deep Sea Res. Oceanogr. Abstr.*, *23*(7), 559–582.

Colebrook, J. M. (1979), Continuous plankton records — Seasonal cycles of phytoplankton and copepods in the North Atlantic Ocean and the North Sea, *Mar. Biol. Berlin*, *51*, 23–32, doi:10.1007/BF00389027.

Cushing, D. H. (1975), *Marine Ecology and Fisheries*, 278 pp., Cambridge Univ. Press, London.

Cushing, D. H. (1990), Plankton production and year-class strength in fish populations — An update of the match-mismatch hypothesis, *Adv. Mar. Biol.*, *26*, 249–293, doi:10.1016/S0065-2881(08)60202-3.

Dickson, R. R., P. M. Kelly, J. M. Colebrook, W. S. Wooster, and D. H. Cushing (1988), North winds and production in the eastern North Atlantic, *J. Plankton Res.*, *10*, 151–169, doi:10.1093/plankt/10.1.151.

Doney, S. C. (2006), Oceanography — Plankton in a warmer world, *Nature*, *444*, 695–696, doi:10.1038/444695a.

Dunne, J. P., R. A. Armstrong, A. Gnanadesikan, and J. L. Sarmiento (2005), Empirical and mechanistic models for the particle export ratio, *Global Biogeochem. Cycles*, *19*, GB4026, doi:10.1029/2004GB002390.

Dutkiewicz, S., M. Follows, J. Marshall, and W. W. Gregg (2001), Interannual variability of phytoplankton abundances in the North Atlantic, *Deep Sea Res., Part II*, *48*, 2323–2344, doi:10.1016/S0967-0645(00)00178-8.

Edwards, M., and A. J. Richardson (2004), Impact of climate change on marine pelagic phenology and trophic mismatch, *Nature*, *430*, 881–884, doi:10.1038/nature02808.

Edwards, M., P. Reid, and B. Planque (2001), Long-term and regional variability of phytoplankton biomass in the Northeast Atlantic (1960–1995), *ICES J. Mar. Sci.*, *58*, 39–49, doi:10.1006/jmsc.2000.0987.

Fan, S. M., W. J. Moxim, and H. Levy (2006), Aeolian input of bioavailable iron to the ocean, *Geophys. Res. Lett.*, *33*, L07602, doi:10.1029/2005GL024852.

Follows, M., and S. Dutkiewicz (2001), Meteorological modulation of the North Atlantic spring bloom, *Deep Sea Res., Part II*, *49*, 321–344, doi:10.1016/S0967-0645(01)00105-9.

Fromentin, J. M., and B. Planque (1996), *Calanus* and environment in the eastern North Atlantic. II. Influence of the North Atlantic Oscillation on *C. finmarchicus* and *C. helgolandicus*, *Mar. Ecol. Prog. Ser.*, *134*, 111–118, doi:10.3354/meps134111.

Gaard, E., and K. Nattestad (2002), Feeding, reproduction and seasonal development of *Calanus finmarchicus* in relation to water masses and phytoplankton in the southern Norwegian Sea, *Rep. CM 2002/N:08*, 16 pp., Int. Counc. for the Explor. of the Sea, Copenhagen.

Garcia, H. E., R. A. Locarnini, T. P. Boyer, and J. I. Antonov (2006), World Ocean Atlas 2005, vol. 3, Dissolved Oxygen, Apparent Oxygen Utilization, and Oxygen Saturation, *NOAA Atlas NESDIS*, 63, edited by S. Levitus, 342 pp., NOAA, Silver Spring, Md.

Geider, R. J., H. L. MacIntyre, and T. M. Kana (1997), Dynamic model of phytoplankton growth and acclimation, responses of the balanced growth rate and the chlorophyll a:carbon ratio to light, nutrient-limitation and temperature, *Mar. Ecol. Prog. Ser.*, *148*, 187–200, doi:10.3354/meps148187.

Gifford, D. J., L. M. Fessenden, P. R. Garrahan, and E. Martin (1995), Grazing by microzooplankton and mesozooplankton in the high latitude North Atlantic Ocean — Spring versus summer dynamics, *J. Geophys. Res.*, *100*, 6665–6675, doi:10.1029/94JC00983.

Gillett, N. P., M. R. Allen, R. E. McDonald, C. A. Senior, D. T. Shindell, and G. A. Schmidt (2002), How linear is the Arctic Oscillation response to greenhouse gases?, *J. Geophys. Res.*, *107*(D3), 4022, doi:10.1029/2001JD000589.

Gillett, N. P., H. F. Graf, and T. J. Osborn (2003), Climate change and the North Atlantic Oscillation, in *The North Atlantic Oscillation: Climatic Significance and Environmental Impact*, *Geophys. Monogr. Ser.*, vol. 134, edited by J. W. Hurrell, pp. 193–210, AGU, Washington, D. C.

Ginoux, P., M. Chin, I. Tegen, J. M. Prospero, B. Holben, O. Dubovik, and S. J. Lin (2001), Sources and distributions of dust aerosols simulated with the GOCART model, *J. Geophys. Res.*, *106*, 20,255–20,273, doi:10.1029/2000JD000053.

Gnanadesikan, A., et al. (2006), GFDL's CM2 global coupled climate models. Part II: The baseline ocean simulation, *J. Clim.*, *19*, 675–697, doi:10.1175/JCLI3630.1.

Greene, C. H., and A. J. Pershing (2000), The response of *Calanus finmarchicus* populations to climate variability in the Northwest Atlantic: Basin-scale forcing associated with the North Atlantic Oscillation, *ICES J. Mar. Sci.*, *57*, 1536–1544, doi:10.1006/jmsc.2000.0966.

Griffies, S. M., M. J. Harrison, R. C. Pacanowski, and A. Rosati (2004), A technical guide to MOM4, *Ocean Group Tech. Rep. 5*, Geophys. Fluid Dyn. Lab., Princeton, N. J.

Heath, M. R., et al. (1999), Climate fluctuations and the spring invasion of the North Sea by *Calanus finmarchicus*, *Fish. Oceanogr.*, *8* suppl. 1, 163–176, doi:10.1046/j.1365-2419.1999.00008.x.

Heath, M. R., et al. (2008), Spatial demography of *Calanus finmarchicus* in the Irminger Sea, *Prog. Oceanogr.*, *76*, 39–88, doi:10.1016/j.pocean.2007.10.001.

Henson, S. A., I. Robinson, J. T. Allen, and J. J. Waniek (2006), Effect of meteorological conditions on interannual variability in timing and magnitude of the spring bloom in the Irminger Basin, North Atlantic, *Deep Sea Res., Part I*, *53*, 1601–1615, doi:10.1016/j.dsr.2006.07.009.

Hirche, H. J., T. Brey, and B. Niehoff (2001), A high frequency time series at Ocean Weather ship station M (Norwegian Sea): Population dynamics of *Calanus finmarchicus*, *Mar. Ecol. Prog. Ser.*, *219*, 205–219, doi:10.3354/meps219205.

Hjort, J. (1914), Fluctuations in the great fisheries of Northern Europe, *J. Cons. Cons. Int. Explor. Mer*, *20*, 1–228.

Hurrell, J. W. (1995), Decadal trends in the North Atlantic Oscillation — Regional temperatures and precipitation, *Science*, *269*, 676–679, doi:10.1126/science.269.5224.676.

Koeve, W. (2001), Wintertime nutrients in the North Atlantic — New approaches and implications for new production estimates, *Mar. Chem.*, *74*, 245–260, doi:10.1016/S0304-4203(01)00016-0.

Large, W., and S. Yeager (2004), Diurnal to decadal global forcing for ocean and sea-ice models: The data sets and flux climatologies, *Tech. Note TN-460+STR*, Natl. Cent. for Atmos. Res., Boulder, Colo.

Levy, M., Y. Lehahn, J. M. Andre, L. Memery, H. Loisel, and E. Heifetz (2005), Production regimes in the northeast Atlantic: A study based on Sea-viewing Wide Field-of-view Sensor (SeaWiFS) chlorophyll and ocean general circulation model mixed layer depth, *J. Geophys. Res.*, *110*, C07S10, doi:10.1029/2004JC002771.

Mann, K. H., and K. F. Drinkwater (1994), Environmental influences on fish and shellfish production in the Northwest Atlantic, *Environ. Rev.*, *2*, 16–32.

Marshall, J., H. Johnson, and J. Goodman (2001), A study of the interaction of the North Atlantic Oscillation with ocean circulation, *J. Clim.*, *14*, 1399–1421, doi:10.1175/1520-0442(2001)014<1399:ASOTIO>2.0.CO;2.

McClain, C. R., S. R. Signorini, and J. R. Christian (2004), Subtropical gyre variability observed by ocean-color satellites, *Deep Sea Res., Part II*, *51*, 281–301, doi:10.1016/j.dsr2.2003.08.002.

McQuatters-Gollop, A., D. E. Raitsos, M. Edwards, Y. Pradhan, L. D. Mee, S. J. Lavender, and M. J. Attrill (2007), A long-term chlorophyll dataset reveals regime shift in North Sea phytoplankton biomass unconnected to nutrient levels, *Limnol. Oceanogr.*, *52*, 635–648.

Mei, Z. P., et al. (2002), Physical control of spring-summer phytoplankton dynamics in the North Water, April–July 1998, *Deep Sea Res., Part II*, *49*, 4959–4982, doi:10.1016/S0967-0645(02)00173-X.

Mignot, J., and C. Frankignoul (2005), The variability of the Atlantic meridional overturning circulation, the North Atlantic Oscillation and the El Niño-Southern Oscillation in the Bergen climate model, *J. Clim.*, *18*, 2361–2375, doi:10.1175/JCLI3405.1.

Ohman, M. D., and H. J. Hirche (2001), Density dependent mortality in an oceanic copepod population, *Nature*, *412*, 638–641, doi:10.1038/35088068.

Osborn, T. J. (2002), The winter North Atlantic Oscillation: Roles of internal variability and greenhouse gas forcing, *CLIVAR Exch.*, *25*, 54–58.

Ottersen, G., and N. C. Stenseth (2001), Atlantic climate governs oceanographic and ecological variability in the Barents Sea, *Limnol. Oceanogr.*, *46*, 1774–1780.

Planque, B., and P. C. Reid (1998), Predicting the abundance of *Calanus finmarchicus* from a climatic signal, *J. Mar. Biol. Assoc. U. K.*, *78*, 1015–1018.

Planque, B., and A. H. Taylor (1998), Long-term changes in zooplankton and the climate of the North Atlantic, *ICES J. Mar. Sci.*, *55*, 644–654, doi:10.1006/jmsc.1998.0390.

Platt, T., C. Fuentes-Yaco, and K. T. Frank (2003), Spring algal bloom and larval fish survival, *Nature*, *423*, 398–399, doi:10.1038/423398b.

Polovina, J. J., E. A. Howell, and M. Abecassis (2008), Ocean's least productive waters are expanding, *Geophys. Res. Lett.*, *35*, L03618, doi:10.1029/2007GL031745.

Reid, P. C. (2005), Atlantic wide regime shift?, *GLOBEC Newsl.*, *11*, 9–10.

Reid, P. C., M. Edwards, H. G. Hunt, and A. J. Warner (1998), Phytoplankton change in the North Atlantic, *Nature*, *391*, 546, doi:10.1038/35290.

Riley, G. A. (1957), Phytoplankton of the North Central Sargasso Sea, *Limnol. Oceanogr.*, *2*, 252–270.

Sameoto, D. (2001), Decadal changes in phytoplankton color index and selected calanoid copepods in continuous plankton recorder data from the Scotian Shelf, *Can. J. Fish. Aquat. Sci.*, *58*, 749–761, doi:10.1139/cjfas-58-4-749.

Siegel, D. A., S. C. Doney, and J. A. Yoder (2002), The North Atlantic spring phytoplankton bloom and Sverdrup's critical depth hypothesis, *Science*, *296*, 730–733, doi:10.1126/science.1069174.

Sunda, W. G., and S. A. Huntsman (1997), Interrelated influence of iron, light and cell size on marine phytoplankton growth, *Nature*, *390*, 389–392, doi:10.1038/37093.

Sverdrup, H. U. (1953), On conditions for the vernal blooming of phytoplankton, *J. Cons. Cons. Int. Explor. Mer*, *18*, 287–295.

Ulbrich, U., and M. Christoph (1999), A shift of the NAO and increasing storm track activity over Europe due to anthropogenic greenhouse gas forcing, *Clim. Dyn.*, *15*, 551–559, doi:10.1007/s003820050299.

Visbeck, M., E. P. Chassignet, R. G. Curry, T. L. Delworth, R. R. Dickson, and G. Krahmann (2003), The ocean's response to North Atlantic Oscillation variability, in *The North Atlantic Oscillation: Climatic Significance and Environmental Impact*, *Geophys. Monogr. Ser.*, vol. 134, edited by J.W. Hurrell, pp. 113–146, AGU, Washington, D. C.

Waniek, J. J., N. P. Holliday, R. Davidson, L. Brown, and S. A. Henson (2005), Freshwater control of onset and species composition of Greenland shelf spring bloom, *Mar. Ecol. Prog. Ser.*, *288*, 45–57, doi:10.3354/meps288045.

Warner, A. J., and G. C. Hays (1994), Sampling by the Continuous Plankton Recorder survey, *Prog. Oceanogr.*, *34*, 237–256, doi:10.1016/0079-6611(94)90011-6.

J. P. Dunne, NOAA Geophysical Fluid Dynamics Laboratory, Princeton, P.O. Box 308, NJ 08544, USA.

S. A. Henson (corresponding author) and J. L. Sarmiento, Atmospheric and Oceanic Sciences Program, Princeton University, Princeton, NJ 08544, USA. (shenson@princeton.edu)